Journal of Engineering Mathematics **48:** 1–26, 2004.

Mud removal and cement placement during primary cementing of an oil well

Part 2; steady-state displacements

S. PELIPENKO[1] and I.A. FRIGAARD[2,*]
[1]*Etudes et Productions Schlumberger, 1, rue Becquerel, 92140 Clamart - France. (e-mail: spelipenko@clamart.oilfield.slb.com)*
[2]*Department of Mathematics and Department of Mechanical Engineering, University of British Columbia, 2324 Main Mall, Vancouver, BC, Canada, V6T 1Z4. (e-mail: frigaard@math.ubc.ca)*

Received 21 August 2002; accepted in revised form 1 May 2003

Abstract. Uncontrolled flows of reservoir fluids behind the casing are relatively common in primary cementing and can lead to any of the following: blowout, leakage at surface, destruction of subsurface ecology, potential contamination of freshwater, delayed or prevented abandonment, as well as loss of revenue due to reduced reservoir pressures. One significant potential cause is ineffective mud removal during primary cementing. Ideally, the drilling mud is displaced all around the annulus and the displacement front advances steadily up the well at the pumping velocity. This paper addresses the question of whether or not such steady-state displacements can be found for a given set of process parameters.

Key words: displacement flows, Hele-Shaw cell, steady states, variational methods, viscoplastic fluid flow

1. Introduction

Primary cementing is a critically important operation in the construction of any oil well, [1, 2]. In this process, a steel casing is cemented into the borehole by pumping a sequence of fluids, (*e.g.*, wash, spacer, cement slurry), down the inside of the casing, returning upwards in the annulus, see Figure 1. The purpose of this operation is to provide a continuous impermeable hydraulic seal in the annulus, preventing any uncontrolled flow of reservoir fluids behind the casing. Many serious problems can arise from uncontrolled flows. Gas or oil may flow to surface causing a blowout, with consequent environmental damage and possible loss of life. Reservoir fluids may migrate into a subsurface aquifer causing contamination of drinking water, or affecting near-wellbore ecology. Finally, even when surface casing vent flows are contained within the annulus, the fact of having pressure at surface prevents a well from being permanently abandoned, (*i.e.*, safely), at the end of its lifetime. Instead, these wells become permanently shut-in and remain an environmental risk. From the financial perspective, an hydraulic connection between different fluid-bearing zones tends to equilibrate pressures. If the zone that is initially at high pressure is an oil or gas-bearing zone, then the reservoir pressure will decrease as it equilibrates. In this case, significant losses in well productivity are common, and it is the consequent loss of revenue that provides a major motivation to oil companies for ensuring that primary cementing is effectively executed.

A widely cited industry figure, *e.g.* [3], is that 15% of primary cementing jobs carried out in the US fail and that about $1/3$ of these failures are due to gas or fluid migration. This problem

*Corresponding author.

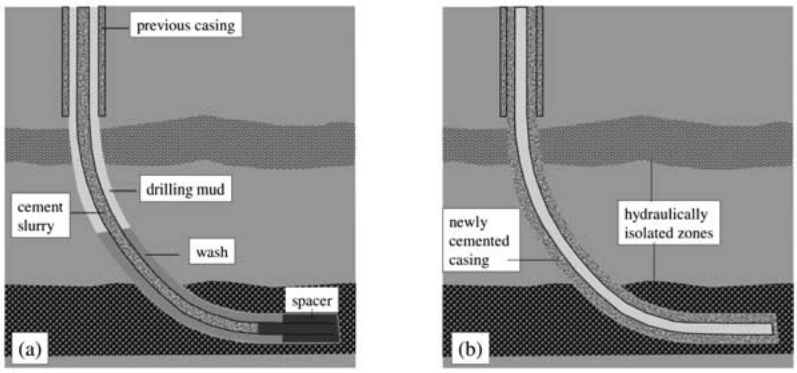

Figure 1. Schematic of the primary cementing process: (a) during and (b) after cementing a new casing.

exists worldwide, (*e.g.*, about 9000 wells are suspended or temporarily abandoned in the U.S. Gulf Coast region). It is also particularly acute in Western Canada, where around 34,000 wells are currently shut-in and suspended, [4]. These are wells that cannot be permanently abandoned due to gas pressures at surface, between the casing and formation, in the cement. Local variations in this problem can be extreme. For example, field survey results are reported in [5], from Tangleflags, Wildmere and Abbey, (three areas in Eastern Alberta). Over a number of years, 0–12% (Tangleflags), 0–15% (Wildmere), and 80% (Abbey) of wells are known to have been leaking in these regions.

One known cause of surface casing vent flows is that the cement, which is placed in the annulus between the outside of the casing and the inside of the hole, fails to fully displace the drilling mud that initially occupies this space. Most commonly, a channel of mud can be left behind on the narrow (lower) side of the annulus, [6–8]. As the cement sets, the mud channel becomes dehydrated and porous, allowing reservoir fluids to flow behind the casing along the annulus. This problem, and the consequences described above, provide the main motivation for this paper.

Although various rule-based systems have been developed, *e.g.*, [9, 10], to aid in designing reliable cementing displacements, and these are routinely applied, *e.g.* [11–13], they fall far short of providing a complete quantitative description of the process. Such systems are phenomenological in approach and rely usually on an analogy with hydraulic systems. Equally, it is not really feasible to model three-dimensional displacements along the entire wellbore using computational fluid dynamics software. This is partly because such software does not cope well with complex displacements, but also because the dimensions of the well, (*i.e.*, very long), make uniform accuracy difficult to achieve.

An intermediate approach to modelling primary cementing is adopted in [14], and it is this approach that we follow here. The model derived in [14] is based on Hele-Shaw approach; its roots may be found in [15], although there the approach is via a porous media analogy. Partial validation and other related experimental work is described in [16, 17].

This paper is effectively *part 2* of [14]. Here we develop further the model in [14], with a view to partly addressing the problem of mud-channelling. Ignoring the possibility of leaks to the surrounding formations, whatever fluids are pumped down the inside of the casing end up in the annulus. A sufficient condition, to avoid the problem of mud channelling, is that the displacement proceeds steadily along the annulus in the upwards axial direction, at the mean

velocity pumped. This paper addresses the important question of whether or not steady-state displacement profiles can exist in the annulus, *i.e.*, travelling-wave solutions.

In the model derived in [14] all variables are averaged across the annular gap, eliminating radial velocities. The model consists of a nonlinear elliptic equation for the stream function and a sequence of advection equations for the fluid concentration. The fluids considered are viscoplastic, meaning here that they will not flow in a narrow channel unless a certain pressure gradient is exceeded, (sufficient for the fluid to yield). The kernel of the stream-function equation becomes infinite at points where the fluids do not yield. This is effectively a Hele-Shaw approach. As such, these flows are very similar mathematically to a class of *viscoplastic* porous-media flows studied by Entov and co-workers, [18, pp. 44–51, 197–222], [19], *i.e.*, those in which there is a limiting pressure gradient, (see also [20] for the origin of this idea).

As a Hele-Shaw displacement problem, there are of course also analogies with classical studies of viscous fingering, [21–23], and their more recent non-Newtonian studies; see for example [24–29]. However, the current paper is not focused on instability and viscous fingering, for a number of reasons. First, in these studies the basic displacement flow is typically a planar displacement, whereas here the basic flow is not obvious. Indeed, finding the basic flow is the aim of this paper. Secondly, typical cementing displacements are designed in a sensible way, *i.e.*, heavy viscous fluid displaces upwards the lighter less viscous fluid. Thus, although instabilities will occur, they may not be *classical* fingering instabilities. Finally, viscous-fingering studies are generally local, which have limited relevance over the length-scale of a typical oil well.

A brief outline is as follows. In Section 2 we present an outline of the model given in part 1 of [14], and extend this to the case where a distinct interface separates the different fluids; Section 2.1. Section 3 establishes the existence of a solution to the stream-function equation, for quite arbitrary and realistic displacements. Steady-state solutions are introduced in Section 4, and we develop analytical solutions for both fully concentric and mildly eccentric annuli, via a perturbation method. Variations in the shapes with the process parameters are also explored. The paper concludes with a short discussion.

2. Model outline

This paper analyses the model for primary cementing derived in [14]. Only half of the annulus is considered and it is assumed that the flow is symmetric with the narrow side corresponding to the lower part of the annulus. Dimensionless spatial coordinates are $(\phi, \xi) \in (0, 1) \times (0, Z)$, where ϕ is the azimuthal coordinate; $\phi = 0$ denotes the *wide side* of the narrow eccentric annular space and $\phi = 1$ denotes the *narrow side*. The ξ coordinate measures axial depth upwards from bottom-hole ($\xi = 0$) to the top of the zone of interest $\xi = Z$, where $Z \gg 1$. The radial coordinate, across the annular gap, has been suppressed in the model derivation, by a combination of scaling arguments and averaging. Application of these methods is motivated by the fact that in a typical oil well,

$$[\text{annular gap}] \ll [\text{annular circumference}] \ll [\text{axial length-scale}],$$

is usually satisfied. The scaling arguments and averaging in [14] are essentially a lubrication/Hele-Shaw modelling approach. The annular gap half-width is denoted $H(\phi, \xi)$:

$$H(\phi, \xi) = \bar{H}(\xi)(1 + e(\xi) \cos \pi\phi),$$

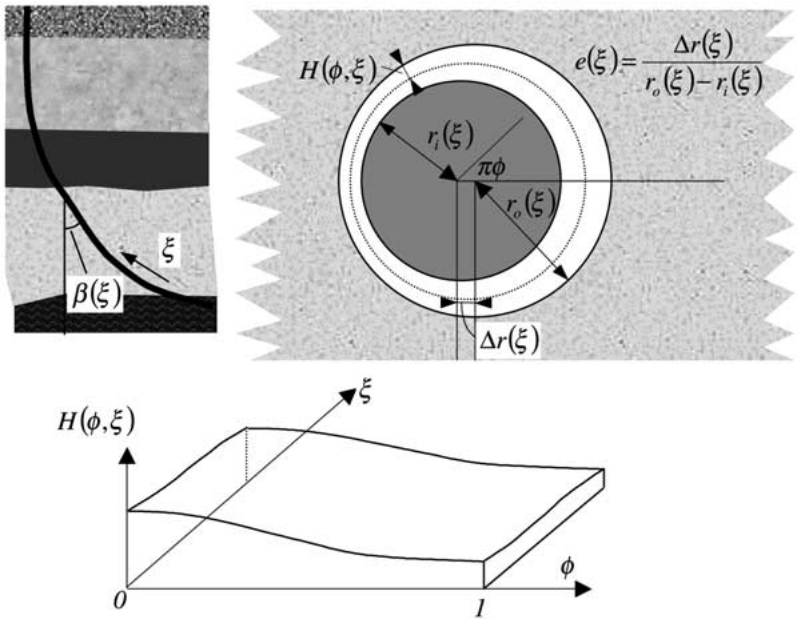

Figure 2. Geometry of the narrow eccentric annulus, mapped to the Hele-Shaw cell geometry.

where $e(\xi) \in [0, 1)$ is the eccentricity; ($e(\xi) = 0$, is concentric and $e(\xi) = 1$, implies that the casing contacts the wellbore wall on the narrow side, which we disallow). The mean annular radius at each depth is denoted by $r_a(\xi)$ and the inclination from vertical is $\beta(\xi)$. It is assumed that the annular geometry, (*i.e.*, $\bar{H}(\xi)$, $e(\xi)$, $r_a(\xi)$ and $\beta(\xi)$), varies slowly in the ξ-direction, see Figure 2.

The flows we consider are therefore two-dimensional and the flow variables have been averaged across the annular gap $H(\phi, \xi)$. The continuity equation is simply

$$\frac{\partial}{\partial\phi}[H\overline{v}] + \frac{\partial}{\partial\xi}[Hr_a\overline{w}] = 0, \tag{1}$$

where $\overline{v}$ and $\overline{w}$ are the averaged velocities in the azimuthal and the axial directions, respectively. This prompts definition of a stream function Ψ:

$$\frac{\partial\Psi}{\partial\phi} = Hr_a\overline{w}, \qquad \frac{\partial\Psi}{\partial\xi} = -H\overline{v}. \tag{2}$$

As is common in a Hele-Shaw model, the (gap-averaged) velocity field is parallel to the (modified) pressure gradient. We consider only laminar flows, and in this case the relationship between the mean speed and the magnitude of the modified pressure gradient, G, is found directly by considering a Poiseuille flow through a plane channel of separation $2H$. For a Newtonian fluid, this relationship can be expressed as:

$$|\nabla_a\Psi| = \frac{H^3G}{3\mu}, \tag{3}$$

where μ denotes the viscosity and ∇_a is defined by:

$$\nabla_a q = \left(\frac{1}{r_a(\xi)}\frac{\partial q}{\partial\phi}, \frac{\partial q}{\partial\xi}\right), \qquad \boldsymbol{\nabla}_a \cdot \boldsymbol{q} = \frac{1}{r_a(\xi)}\frac{\partial q_\phi}{\partial\phi} + \frac{\partial q_\xi}{\partial\xi}.$$

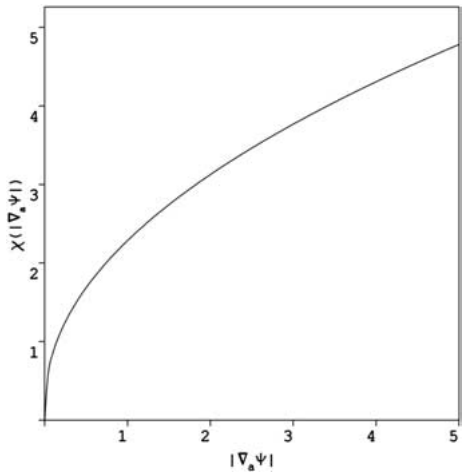

Figure 3. The function $\chi(|\nabla_a\Psi|; H, \tau_Y, \kappa, m)$, for parameters $\tau_Y = \kappa = H = 1{\cdot}0$, $m = 1/n = 2{\cdot}0$.

However, the fluids that we consider are characterised as Herschel-Bulkley fluids, with a yield stress τ_Y, consistency κ and power-law index n. If the magnitude of the modified pressure gradient, G, does not exceed a critical value, τ_Y/H, the fluid is unyielded at the walls and does not flow.[1] The excess of the pressure gradient over this critical value is denoted χ:

$$\chi = G - \frac{\tau_Y}{H}. \tag{4}$$

The relationship between areal flow rate, $|\nabla_a\Psi|$, and χ is:

$$|\nabla_a\Psi| = \begin{cases} 0 & \chi \le 0, \\ \dfrac{H^{m+2}}{\kappa^m(m+2)} \dfrac{\chi^{m+1}}{(\chi+\tau_Y/H)^2}\left[\chi + \dfrac{(m+2)\tau_Y}{(m+1)H}\right] & \chi > 0, \end{cases} \tag{5}$$

where $m = 1/n$, which reduces to (3) when $n = 1$, $\tau_Y = 0$ and $\kappa = \mu$. The function χ is defined implicitly as a function of $|\nabla_a\Psi|$, by (5). Clearly also we have $\chi = \chi(|\nabla_a\Psi|; H, \tau_Y, \kappa, m)$, but we shall be most concerned with the dependence of χ on $|\nabla_a\Psi|$. In general, χ is a positive increasing function of $|\nabla_a\Psi|$. An example of this dependence is shown in Figure 3. Further properties of $\chi = \chi(|\nabla_a\Psi|)$ are explored in Section 3.2.1.

The following coupled system of partial differential equations is derived in [14]:

$$\frac{\partial}{\partial t}[Hr_a\overline{c}_k] + \frac{\partial}{\partial\phi}[H\overline{v}\,\overline{c}_k] + \frac{\partial}{\partial\xi}[Hr_a\overline{w}\,\overline{c}_k] = 0, \quad k = 1, 2, ..., K \tag{6}$$

$$\nabla_a \cdot \boldsymbol{S} = -f, \tag{7}$$

A sequence of K fluids is pumped around the wellbore, each with a (radially-averaged) concentration $\overline{c}_k$. Diffusive and dispersive effects are negligible compared to advection. The velocities $\overline{v}$ and $\overline{w}$, in the advection equations (6), are computed from the stream function Ψ, via (2). The stream function Ψ is determined from solution of (7) which is coupled with the following visco-plastic constitutive laws (8) and (9):

$$\boldsymbol{S} = \left[\frac{r_a\chi(|\nabla_a\Psi|)}{|\nabla_a\Psi|} + \frac{r_a\tau_Y}{H|\nabla_a\Psi|}\right]\nabla_a\Psi \iff |S| > \frac{r_a\tau_Y}{H}, \tag{8}$$

$$|\nabla_a \Psi| = 0 \Longleftrightarrow |S| \leq \frac{r_a \tau_Y}{H}. \tag{9}$$

These have been derived by consideration of a Poiseuille flow of an Herschel-Bulkley fluid through a slot of local half-width H. The term f in (7) contains the buoyancy terms, given by:

$$f = \nabla_a \cdot \left(\frac{r_a \rho(\overline{\boldsymbol{c}}) \cos\beta}{\mathrm{St}^*}, \frac{r_a \rho(\overline{\boldsymbol{c}}) \sin\beta \sin\pi\phi}{\mathrm{St}^*} \right) = \nabla_a \cdot \tilde{\boldsymbol{f}}, \tag{10}$$

where the parameter St^* is a Stokes number for the displacement flow.

As boundary conditions for (6), we impose the condition of symmetry at the wide and narrow sides:

$$\frac{\partial \overline{c}_k}{\partial \phi} = 0, \qquad \phi = 0, 1. \tag{11}$$

At $\xi = 0$, we impose either $\overline{c}_k = 0$ or $\overline{c}_k = 1$, according to which fluid is entering the annulus. Equation (7) is essentially an elliptic second-order equation. On the wide side of the annulus we impose,

$$\Psi(0, \xi, t) = 0. \tag{12}$$

and on the narrow side, since the flow is incompressible, we have:

$$\Psi(1, \xi, t) = Q(t), \tag{13}$$

where $Q(t)$ is the dimensionless flow rate. At the ends of the annulus we impose Dirichlet conditions:

$$\Psi(\phi, 0, t) = \Psi_0(\phi, t), \qquad \Psi(\phi, Z, t) = \Psi_Z(\phi, t), \tag{14, 15}$$

although we note that suitable functions $\Psi_0(\phi, t)$ & $\Psi_Z(\phi, t)$ are not always easy to specify.

2.1. Interface-tracking formulation

We note in (6) that each fluid concentration is simply advected through the annulus. Since the inflow concentrations will be specified as either 0 or 1, there is no theoretical possibility for intermediate concentrations to evolve, (although numerically this will happen). It is therefore tempting to track the interface between fluid domains instead of solving (6). Certainly, in considering steady-state displacement solutions analytically, (in Section 4), it is far simpler to work with an interface position than with a concentration gradient.

It is relatively straightforward to develop an interface-tracking formulation, using similar approximations to those made in [14]. For simplicity, we consider only two fluids and divide the domain $\Omega = (0, 1) \times (0, Z)$ into two fluid domains: Ω_1 for the displacing (lower) fluid 1, and Ω_2 for the displaced (upper) fluid 2. Following the procedure in [14] for this two-fluid problem, (7) becomes:

$$\nabla_a \cdot \boldsymbol{S}_1 = 0, \qquad (\phi, \xi) \in \Omega_1; \qquad\qquad \nabla_a \cdot \boldsymbol{S}_2 = 0, \qquad (\phi, \xi) \in \Omega_2, \tag{16, 17}$$

with $\boldsymbol{S}_1$ and $\boldsymbol{S}_2$ defined as in (8–9), with properties $\rho_1, \tau_{1,Y}, \kappa_1, m_1$ in fluid 1 and $\rho_2, \tau_{2,Y}, \kappa_2, m_2$ in fluid 2. Note from (10) that in each single fluid domain there are no density gradients and thus $f = 0$, (we neglect all ξ-derivatives of the geometrical parameters).

The starting point for modelling the interface evolution is a kinematic equation. After applying scaling arguments and averaging across the gap, we obtain the kinematic condition for the interface, denoted by $\xi = h(\phi, t)$, as follows:

$$\frac{\partial h}{\partial t} + \frac{\bar{v}}{r_a}\frac{\partial h}{\partial \phi} = \bar{w}, \tag{18}$$

which replaces (6). The leading-order continuity conditions at the interface are that the pressure p and the stream function Ψ are continuous across the interface:

$$\left[p\right]_1^2 = 0, \qquad [\Psi]_1^2 = 0, \tag{19, 20}$$

where $[q]_1^2$ denotes the difference in q between fluid 2 and fluid 1 across the interface. Since (16) and (17) involve only Ψ, we would like to replace the pressure in (19) with a closure relation involving only Ψ. From [14] we can express $\boldsymbol{S}_k$ as:

$$\boldsymbol{S}_k = (S_{k,\phi}, S_{k,\xi}) \equiv \left(-r_a\frac{\partial p}{\partial \xi} - \frac{\rho_k r_a \cos\beta}{\mathrm{St}^*}, \frac{\partial p}{\partial \phi} - \frac{\rho_k r_a \sin\beta \sin\pi\phi}{\mathrm{St}^*}\right). \tag{21}$$

If smoothness of the interface is assumed, the tangential derivative of p along the interface will also be continuous:

$$\left[\boldsymbol{t}\cdot\nabla_a p\right]_1^2 = \left[\frac{1}{r_a}\frac{\partial p}{\partial \phi} + \frac{\partial p}{\partial \xi}\frac{\partial h}{\partial \phi}\right]_1^2 = 0 \tag{22}$$

where $\boldsymbol{t} = (1, \frac{\partial h}{\partial \phi})$. Equation (22) allows us to use (8) and (21) to eliminate the pressure, *i.e.*,

$$\left[\left(\frac{\chi_k + \dfrac{\tau_{k,Y}}{H}}{|\nabla_a \Psi|}\right)\left(\frac{\partial \Psi}{\partial \xi} - \frac{1}{r_a}\frac{\partial \Psi}{\partial \phi}\frac{\partial h}{\partial \phi}\right) + \left(\frac{\rho_k \sin\beta\sin\pi\phi}{\mathrm{St}^*} - \frac{\rho_k\cos\beta}{\mathrm{St}^*}\frac{\partial h}{\partial \phi}\right)\right]_1^2 = 0, \tag{23}$$

which expresses (22) in terms of Ψ. Note that, strictly speaking, (23) is valid only if both fluids are yielded at the interface, *i.e.*, if $|S_k| > r_a\tau_{k,Y}/H$. Below the yield stress $\boldsymbol{S}_k$, and consequently the pressure, are indeterminate and the more general form of (23) is:

$$\left[\left(\frac{S_{k,\xi}}{r_a} - \frac{S_{k,\phi}}{r_a}\frac{\partial h}{\partial \phi}\right) + \left(\frac{\rho_k \sin\beta\sin\pi\phi}{\mathrm{St}^*} - \frac{\rho_k\cos\beta}{\mathrm{St}^*}\frac{\partial h}{\partial \phi}\right)\right]_1^2 = 0, \tag{24}$$

which we will use later. Note that (23) describes the jump in the normal derivative of Ψ at the interface. Finally we note that, by differentiating (20) along the interface, we have:

$$[\boldsymbol{t}\cdot\nabla_a\Psi]_1^2 = \left[\frac{1}{r_a}\frac{\partial \Psi}{\partial \phi} + \frac{\partial \Psi}{\partial \xi}\frac{\partial h}{\partial \phi}\right]_1^2 = 0, \tag{25}$$

which is equivalent to the continuity of the normal component of velocity, which is required for the velocities in (18) to be well-defined.

3. Existence of a unique Ψ

In Section 4 we consider whether there exist steady-state solutions to (7), using the formulation above in Section 2.1. These solutions advance along the annulus at the mean pumping speed of the fluid: $Q/[r_a\bar{H}]$ and such solutions provide the overall focus for the paper. However, first we consider a broader question: whether or not there exist solutions to Equation (7), with the specified boundary conditions and for reasonable model data? In this section, we answer this question in the affirmative, for either the formulation leading to the concentration

equation (6), or for that in Section 2.1, *i.e.*, for a broad range of practical conditions it is possible to find a unique solution to (7). This minimal knowledge should suffice for the reader who does not wish to delve overly into mathematical detail and who may now proceed directly to Section 4.

To motivate our study of (7), we remark that Equation (6) is simply an advection equation for the concentration, as is the kinematic equation. Thus, in either formulation the fluids are simply advected along according to the streamlines Ψ. The stream function is determined from the elliptic problem (7), (or from (16) and (17)), and time only enters in the specification of the flow rate $Q(t)$ as the narrow side boundary condition. Thus, computing the stream function decouples from the time advance of the concentrations and interface. A natural problem, therefore, is to assume a realistically regular interface, (or concentration field), and examine under what conditions a unique stream-function solution exists. For the remainder of this section we therefore ignore (6), (or the kinematic condition), and consider Ψ alone.

Our approach in the sequel is to use classical results from variational methods and convex analysis. The aim is to show that a weak form of (7) can be re-cast as a minimisation problem, which we know has a unique solution. The reader unfamiliar with these methods is referred to [30, 31], or to [32, pp. 278–326], [33, pp. 78–95], for examples of similar applications.

3.1. VARIATIONAL FORMULATION

Observe that the classical formulations that we have derived above are not necessarily well-defined, due to the unyielded regions of the annulus, (where $|S| \leq r_a \tau_Y / H$), being unspecified. Therefore, here we derive a formulation that can be handled more rigorously. We proceed purely formally, assuming sufficient regularity of our solution and the test functions that we use. We treat first the fluid mixture formulation and then the interface-tracking formulation, showing that both formulations may be described by the same variational inequality.

3.1.1. *Fluid-mixture formulation*

We start with the field equation (7), boundary conditions (12–15) and the constitutive laws (8) and (9). There is no time dependency and thus we consider that a concentration field is defined throughout Ω. This concentration field is used to define the fluid-mixture properties via a set of constitutive laws for each property. The constitutive laws are unspecified but we do impose the (physically justifiable) restrictions that: $\rho > 0$, $\tau_Y \geq 0$, $\kappa > 0$, $m > 0$. We also suppose that these constitutive laws are smooth. Thus, we may consider that each of ρ, τ_Y, κ, m vary with (ϕ, ξ).

We commence by homogenizing the boundary conditions by setting[2]

$$\Psi = \Psi^* + u : \qquad u \in C_0^\infty(\Omega). \tag{26}$$

Now let $v,\ w \in C_0^\infty(\Omega)$, with $w = v - u$. Then, from (7) and using the divergence theorem, we have:

$$\int_\Omega f w \, \mathrm{d}\Omega = \int_\Omega \boldsymbol{S} \cdot \nabla_a w \, \mathrm{d}\Omega - \oint_{\partial\Omega} w \boldsymbol{S} \cdot \boldsymbol{n} \, \mathrm{d}s = \int_\Omega \boldsymbol{S} \cdot \nabla_a w \, \mathrm{d}\Omega. \tag{27}$$

Consider the integrand on the right-hand side of (27). Firstly, if the fluid is yielded, $|\boldsymbol{S}| > r_a \tau_Y / H$:

$$\begin{aligned}
\boldsymbol{S}\cdot\nabla_a w &= \frac{r_a\chi(|\nabla_a\Psi^*+\nabla_a u|)}{|\nabla_a\Psi^*+\nabla_a u|}(\nabla_a\Psi^*+\nabla_a u)\cdot(\nabla_a v-\nabla_a u)\\
&\quad+\frac{\tau_Y r_a}{H}\frac{(\nabla_a\Psi^*+\nabla_a u)\cdot(\nabla_a v-\nabla_a u)}{|\nabla_a\Psi^*+\nabla_a u|}\\
&\leq \frac{r_a\chi(|\nabla_a\Psi^*+\nabla_a u|)}{|\nabla_a\Psi^*+\nabla_a u|}(\nabla_a\Psi^*+\nabla_a u)\cdot(\nabla_a v-\nabla_a u)\\
&\quad+\frac{\tau_Y r_a}{H}(|\nabla_a\Psi^*+\nabla_a v|-|\nabla_a\Psi^*+\nabla_a u|),
\end{aligned}\tag{28}$$

using the Cauchy-Schwarz inequality. Secondly, if the fluid is unyielded, $|\boldsymbol{S}|\leq r_a\tau_Y/H$, then $\nabla_a\Psi=\nabla_a\Psi^*+\nabla_a u=0$, and

$$\begin{aligned}
\boldsymbol{S}\cdot\nabla_a w &= \boldsymbol{S}\cdot\left[(\nabla_a\Psi^*+\nabla_a v)-(\nabla_a\Psi^*+\nabla_a u)\right]\leq|\boldsymbol{S}||\nabla_a\Psi^*+\nabla_a v|\\
&\leq \frac{\tau_Y r_a}{H}|\nabla_a\Psi^*+\nabla_a v|\leq\frac{r_a\chi(|\nabla_a\Psi^*+\nabla_a u|)}{|\nabla_a\Psi^*+\nabla_a u|}(\nabla_a\Psi^*+\nabla_a u)\cdot(\nabla_a v-\nabla_a u)\\
&\quad+\frac{\tau_Y r_a}{H}(|\nabla_a\Psi^*+\nabla_a v|-|\nabla_a\Psi^*+\nabla_a u|).
\end{aligned}\tag{29}$$

Finally, using (10) and the divergence theorem, we see that a classical solution of the mixture formulation, will satisfy:

$$\begin{aligned}
&\int_\Omega\frac{r_a\chi(|\nabla_a\Psi^*+\nabla_a u|)}{|\nabla_a\Psi^*+\nabla_a u|}(\nabla_a\Psi^*+\nabla_a u)\cdot(\nabla_a v-\nabla_a u)\\
&\quad+\frac{\tau_Y r_a}{H}(|\nabla_a\Psi^*+\nabla_a v|-|\nabla_a\Psi^*+\nabla_a u|)+\tilde{\boldsymbol{f}}\cdot\nabla_a(v-u)\mathrm{d}\Omega\geq 0.
\end{aligned}\tag{30}$$

where $\tilde{\boldsymbol{f}}$ is defined in (10).

3.1.2. *Interface-tracking formulation*

Here we start with the field equations (16) and (17), the constitutive laws (8) and (9), boundary conditions (12–15), and the continuity conditions (20) and (24) at the interface. For simplicity, in our derivation we assume that only two fluids are present in the annulus, the generalisation to K fluids being straightforward. Again we multiply (16) and (17) by a test function $w\in C_0^\infty(\Omega)$ and integrate over each sub-domain:

$$\int_{\Omega_1}\boldsymbol{S}_1\cdot\nabla_a w\,\mathrm{d}\Omega_1+\int_{\Omega_2}\boldsymbol{S}_2\cdot\nabla_a w\,\mathrm{d}\Omega_2=\oint_{\partial\Omega_1}w\boldsymbol{S}_1\cdot\boldsymbol{n_1}\,\mathrm{d}s+\oint_{\partial\Omega_2}w\boldsymbol{S}_2\cdot\boldsymbol{n_2}\,\mathrm{d}s\tag{31}$$

corresponding to (27). It is assumed that the interface is Lipschitz continuous for the above to make sense. The boundary-integral terms on the right-hand side vanish, except along the interface between the two fluids, denoted Γ, where we have

$$\oint_{\partial\Omega_1}w\boldsymbol{S}_1\cdot\boldsymbol{n_1}\,\mathrm{d}s+\oint_{\partial\Omega_2}w\boldsymbol{S}_2\cdot\boldsymbol{n_2}\,\mathrm{d}s=\int_\Gamma w(\boldsymbol{S}_1-\boldsymbol{S}_2)\cdot\boldsymbol{n_1}\,\mathrm{d}s.\tag{32}$$

Substituting for $\boldsymbol{S}_k$ and using (24):

$$[\boldsymbol{S}_1-\boldsymbol{S}_2]\cdot\boldsymbol{n_1}=-[\tilde{\boldsymbol{f}}_1-\tilde{\boldsymbol{f}}_2]\cdot\boldsymbol{n_1}\tag{33}$$

where

$$\tilde{\boldsymbol{f}}_{\boldsymbol{k}} = \left(\frac{\rho_k \cos\beta r_a}{\mathrm{St}^*}, \frac{r_a \rho_k \sin\beta \sin\pi\phi}{\mathrm{St}^*} \right)_j \tag{34}$$

Therefore, using the divergence theorem and noting that $\boldsymbol{\nabla}_a \cdot \tilde{\boldsymbol{f}}_{\boldsymbol{k}} = 0$, we have:

$$\begin{aligned} \int_\Gamma w(\boldsymbol{S}_1 - \boldsymbol{S}_2) \cdot \boldsymbol{n_1} \, \mathrm{d}s &= -\oint_{\partial\Omega_1} w \tilde{\boldsymbol{f}}_{\boldsymbol{1}} \cdot \boldsymbol{n_1} \, \mathrm{d}s - \oint_{\partial\Omega_2} w \tilde{\boldsymbol{f}}_{\boldsymbol{2}} \cdot \boldsymbol{n_2} \, \mathrm{d}s \\ &= -\int_{\Omega_1} \tilde{\boldsymbol{f}}_{\boldsymbol{1}} \cdot \nabla_a w \, \mathrm{d}\Omega_1 - \int_{\Omega_2} \tilde{\boldsymbol{f}}_{\boldsymbol{2}} \cdot \nabla_a w \, \mathrm{d}\Omega_2. \end{aligned} \tag{35}$$

Finally, treating the $\boldsymbol{S}_k \cdot \nabla_a w$ terms as with the mixture formulation, we have:

$$\begin{aligned} &\sum_j \int_{\Omega_j} \frac{r_a \chi(|\nabla_a \Psi^* + \nabla_a u|)}{|\nabla_a \Psi^* + \nabla_a u|} (\nabla_a \Psi^* + \nabla_a u) \cdot (\nabla_a v - \nabla_a u) \\ &\quad + \frac{\tau_Y r_a}{H} (|\nabla_a \Psi^* + \nabla_a v| - |\nabla_a \Psi^* + \nabla_a u|) + \tilde{\boldsymbol{f}}_{\boldsymbol{j}} \cdot \nabla_a (v - u) \, \mathrm{d}\Omega_j \geq 0. \end{aligned} \tag{36}$$

3.2. Existence and uniqueness

The principal advantage of the variational formulation is that the tricky question of determining yielded and unyielded regions is avoided. Secondly, we may consider the two formulations within the same integral framework.

We assume that r_a, β, $e \in L^2(0, Z)$, since the geometry varies slowly along the well. When it is also assumed that the fluid concentration fields are in $L^2(\Omega)$ and that the interface is Lipschitz continuous, it follows that each of ρ, τ_Y, κ, $m \in L^2(\Omega)$, and hence that $\tilde{\boldsymbol{f}} \in [L^2(\Omega)]^2$. This is also physically reasonable. We assume that Ψ^*, $\Psi \in V$ with $u \in V_0$, with V_0 being the subspace of V with $u = 0$ on $\partial\Omega$. The spaces V and V_0 are determined later, but it is evident from (30) and (36) that some weak form of differentiability is required. Thus, these spaces will be closures of subspaces of $C^\infty(\Omega)$ with respect to certain Sobolev norms. Noting the formal equivalence of (30) and (36), we now take

$$\begin{aligned} &\int_\Omega \frac{r_a \chi(|\nabla_a \Psi^* + \nabla_a u|)}{|\nabla_a \Psi^* + \nabla_a u|} (\nabla_a \Psi^* + \nabla_a u) \cdot (\nabla_a v - \nabla_a u) \\ &\quad + \frac{\tau_Y r_a}{H} (|\nabla_a \Psi^* + \nabla_a v| - |\nabla_a \Psi^* + \nabla_a u|) + \tilde{\boldsymbol{f}} \cdot \nabla_a (v - u) \, \mathrm{d}\Omega \geq 0 \\ &\qquad\qquad u \in V_0, \ \forall v \in V_0, \end{aligned} \tag{37}$$

as the weak definition of our problem, *i.e.*, incorporating either formulation. It is apparent that a solution to (37) will also minimise the following functional:

$$J(v) = \int_\Omega \frac{r_a}{2} \int_0^{|\nabla_a \Psi^* + \nabla_a v|^2} \frac{\chi(s^{1/2})}{s^{1/2}} \, \mathrm{d}s + \frac{\tau_Y r_a}{H} |\nabla_a \Psi^* + \nabla_a v| + \tilde{\boldsymbol{f}} \cdot \nabla_a v \, \mathrm{d}\Omega. \tag{38}$$

We now show that the minimization problem

$$J(u) \leq J(v), \forall \, v \in V_0, \ u \in V_0; \tag{39}$$

has a unique solution $u \in V_0$, which solves the original problem in its variational formulation (30). To do this we use classical results from convex analysis. The application of these results and determination of the space in which the solution lies depends largely on the properties of χ. We explore these properties next; in Section 3.2.2 give some preliminary results, and in Section 3.2.3 show the existence and uniqueness of a solution.

3.2.1. *Properties of* χ

Here we are only interested in the properties of χ as a function of $|\nabla_a \Psi|$. Thus, here we write $\chi = \chi(|\nabla_a \Psi|)$ and denote by $\chi'(|\nabla_a \Psi|)$ the partial derivative of $\chi(|\nabla_a \Psi|)$ with respect to $|\nabla_a \Psi|$. Let:

$$A = \frac{H^{m+2}}{\kappa^m (m+2)} > 0; \qquad B = \frac{\tau_Y}{H} > 0.$$

The function χ is defined implicitly by (5). The following properties are established using elementary methods.

1. Asymptotic behavior as $|\nabla_a \Psi| \to 0$:

$$\left| \nabla_a \Psi| \sim \frac{A \chi^{m+1}}{B} \left(\frac{m+2}{m+1} \right) \Rightarrow \chi \sim \left(\frac{B}{A} \frac{(m+1)}{(m+2)} \right)^{1/(m+1)} |\nabla_a \Psi|^{1/(m+1)} \right. \tag{40}$$

2. Asymptotic behavior as $|\nabla_a \Psi| \to \infty$:

$$|\nabla_a \Psi| \sim A \chi^m \Rightarrow \chi \sim A^{-1/m} |\nabla_a \Psi|^{1/m}. \tag{41}$$

3. Derivatives with respect to $|\nabla_a \Psi|$ for $\chi > 0$:

$$\begin{aligned} \frac{\partial |\nabla_a \Psi|}{\partial \chi} &= \frac{A \chi^m}{(\chi + B)^3} \left(m \chi^2 + 2m \frac{(m+2)}{(m+1)} B \chi + (m+2) B^2 \right) > 0 \\ \chi' &= \frac{\partial \chi}{\partial |\nabla_a \Psi|} = \left(\frac{\partial |\nabla_a \Psi|}{\partial \chi} \right)^{-1} > 0 \end{aligned} \tag{42}$$

i.e., χ is strictly increasing.

4. Bounds on χ, for all $|\nabla_a \Psi|$:

$$\chi \geq \left(\frac{m+1}{A(m+2)} \right)^{1/m} |\nabla_a \Psi|^{1/m} \tag{43}$$

$$\chi \leq \begin{cases} \left(\dfrac{2B}{A} \right)^{1/(m+1)} |\nabla_a \Psi|^{1/(m+1)} & |\nabla_a \Psi| \leq A B^m / 2, \\ ] \left(\dfrac{2}{A} \right)^{1/m} |\nabla_a \Psi|^{1/m} & |\nabla_a \Psi| > A B^m / 2, \end{cases} \tag{44}$$

3.2.2. *Preliminary results*

PROPOSITION 1. *Let*

$$\Phi(x,\,y) = \int_0^{x^2+y^2} \frac{\chi(s^{1/2})}{s^{1/2}}\,\mathrm{d}s,$$

with χ as above. Then Φ is strictly convex in $\mathbb{R}^2$.

Proof. The Hessian matrix of Φ is easily computed and has eigenvalues $2\frac{\chi(r)}{r}$ and $2\chi\prime(r)$, both of which are strictly positive. Thus $\Phi(x,\,y)$ is strictly convex in $\mathbb{R}^2$. (Here $r^2 = x^2 + y^2$). □

PROPOSITION 2. *J(v) as defined in (38) is strictly convex.*

Proof. Strict convexity of the first term in $J(v)$ follows directly from Proposition 1. Convexity of the second term in $J(v)$ follows from the triangle inequality. The third term in $J(v)$ is linear in v and hence trivially convex. Thus, $J(v)$ is a sum of two convex functions and a strictly convex function and is itself strictly convex in $\mathbb{R}$. □

Now let us show that $\lim_{||v||\to+\infty} J(v) = +\infty$. Let

$$K(\boldsymbol{x}) = \int_\Omega \frac{r_a}{2}\int_0^{|\boldsymbol{x}|^2} \frac{\chi(s^{1/2})}{s^{1/2}}\,\mathrm{d}s + \frac{\tau_Y r_a}{H}|\boldsymbol{x}| + \tilde{\boldsymbol{f}}\cdot(\boldsymbol{x} - \nabla_a\Psi^*)\,\mathrm{d}\Omega. \tag{45}$$

where $\boldsymbol{x} : \mathbb{R}^2 \to \mathbb{R}^2$ so that $J(v) = K(\nabla_a\Psi^* + \nabla_a v)$.

PROPOSITION 3. *$K(\boldsymbol{x}) \to \infty$ as $\int_\Omega |\boldsymbol{x}|^{1+1/m}\,\mathrm{d}\Omega \to \infty$.*

Proof. From the lower bounds in Section 3.2.1, there exists $\alpha > 0$:

$$\chi \geq \alpha|\nabla_a\Psi|^{1/m}, \tag{46}$$

Thus,

$$\begin{aligned} K(\boldsymbol{x}) &\geq \int_\Omega \frac{\alpha r_a}{2}\int_0^{|\boldsymbol{x}|^2} \frac{s^{1/(2m)}}{s^{1/2}}\,\mathrm{d}s - |\tilde{\boldsymbol{f}}||\boldsymbol{x}| + \tilde{\boldsymbol{f}}\cdot\nabla_a\Psi^*\,\mathrm{d}\Omega \\ &\geq \int_\Omega \frac{\alpha r_a}{1+1/m}|\boldsymbol{x}|^{1+1/m} - |\tilde{\boldsymbol{f}}||\boldsymbol{x}|\,\mathrm{d}\Omega + \delta, \end{aligned} \tag{47}$$

where $\delta = -\int_\Omega \tilde{\boldsymbol{f}}\cdot\nabla_a\Psi^*\,\mathrm{d}\Omega$. Using Hölder's inequality:

$$\begin{aligned} K(\boldsymbol{x}) &\geq \tilde{\alpha}\int_\Omega |\boldsymbol{x}|^{1+1/m}\,\mathrm{d}\Omega - c_*\left[\int_\Omega |\boldsymbol{x}|^{1+1/m}\,\mathrm{d}\Omega\right]^{\frac{1}{1+1/m}} + \delta, \\ &= \tilde{\alpha}\int_\Omega |\boldsymbol{x}|^{1+1/m}\,\mathrm{d}\Omega\left(1 - \frac{c_*}{\tilde{\alpha}}\left[\int_\Omega |\boldsymbol{x}|^{1+1/m}\,\mathrm{d}\Omega\right]^{-\frac{1}{1+m}}\right) + \delta, \\ &\quad\to\infty \ \text{ as } \ \int_\Omega |\boldsymbol{x}|^{1+1/m}\,\mathrm{d}\Omega \to \infty, \end{aligned}$$

where $\tilde{\alpha} = \min(r_a)\alpha/(1+1/m) > 0$, $c_* = \left[\int_\Omega |\tilde{\boldsymbol{f}}|^{p'}\,\mathrm{d}\Omega\right]^{1/p'}$ with $1/p + 1/p' = 1$ and $p = 1 + 1/m$. □

LEMMA 1. *$J(v) \to \infty$ as $||v||_{W^{1,1+1/m}} \to \infty$.*

Proof. We note that for $v \in W_0^{1,1+1/m}(\Omega)$, a Poincaré-type inequality holds, and the seminorm

$$\left[\int_\Omega |\nabla v|^{1+1/m}\right]^{\frac{1}{1+1/m}},$$

is an equivalent norm to $||v||_{W^{1,1+1/m}}$, see for example Theorem 1.7 in [30, Chapter 2]. Secondly, note that as

$$|\nabla_a \Psi^* + \nabla_a v| \geq |\nabla_a v| - |\nabla_a \Psi^*|, \tag{48}$$

we have

$$||v||_{W^{1,1+1/m}(\Omega)} \to \infty \Rightarrow ||\nabla_a \Psi^* + \nabla_a v||_{L_{1+1/m}(\Omega)} \to \infty. \tag{49}$$

The result then follows directly from proposition 3. □

3.2.3. *Existence and uniqueness*

To summarise, $J(v)$ is continuous, strictly convex and $J(v) \to \infty$ as $||v||_{W^{1,1+1/m}(\Omega)} \to \infty$. Thus, as $W_0^{1,1+1/m}(\Omega)$ is a closed convex nonempty subset of $W^{1,1+1/m}(\Omega)$, from standard optimization theory in Banach spaces it follows that the minimization problem (39) has a unique solution $u \in W_0^{1,1+1/m}(\Omega)$, see *e.g.* [31]. Moreover, on writing $J(v) = J_0(v) + J_1(v)$, where

$$J_0(v) = \int_\Omega \frac{r_a}{2} \int_0^{|\nabla_a \Psi^* + \nabla_a v|^2} \frac{\chi(s^{1/2})}{s^{1/2}} \, \mathrm{d}s + \tilde{\boldsymbol{f}} \cdot \nabla_a v \, \mathrm{d}\Omega \tag{50}$$

is strictly convex and Gateaux-differentiable on $W_0^{1,1+1/m}(\Omega)$ and

$$J_1(v) = \int_\Omega \frac{\tau_Y r_a}{H} |\nabla_a \Psi^* + \nabla_a v| \, \mathrm{d}\Omega \tag{51}$$

is convex and continuous, we have (see Theorem 2.1 in Chapter V of [33]) that the unique solution of the minimization problem is characterized by

$$(J_0'(u), v - u) + J_1(v) - J_1(u) \geq 0, \ \forall v \in W_0^{1,1+1/m}(\Omega), \ u \in W_0^{1,1+1/m}(\Omega) \tag{52}$$

where $(J_0'(v), w)$ is the Gateaux derivative of J_0:

$$\begin{aligned}(J_0'(v), w) &= \lim_{t \to 0} \frac{J_0(v + tw) - J_0(v)}{t} \\ &= \int_\Omega \frac{r_a \chi(|\nabla_a \Psi^* + \nabla_a v|)}{|\nabla_a \Psi^* + \nabla_a v|} (\nabla_a \Psi^* + \nabla_a v) \cdot \nabla_a w + \tilde{\boldsymbol{f}} \cdot \nabla_a w \, \mathrm{d}\Omega.\end{aligned}$$

Thus, on substituting in (52), we clearly recover the variational formulation (37). We conclude that the variational formulation has a unique solution in $W_0^{1,1+1/m}(\Omega)$. Furthermore, since $W^{1,1+1/m}(\Omega)$ is an affine space, *i.e.*,

$$W^{1,1+1/m}(\Omega) = \Psi^* + W_0^{1,1+1/m}(\Omega),$$

for any $\Psi^* \in W^{1,1+1/m}(\Omega)$, (and we have also shown that such a Ψ^* can be constructed), it follows that there exists a unique stream function $\Psi \in W^{1,1+1/m}(\Omega)$.

Remark 1: In proving the above results, for brevity we have been rather negligent in our definition of m. In the mixture formulation, we must assume (as in [14]), that the rheological parameters of the mixture, (*i.e.*, having intermediate concentrations), are defined by closure laws that preserve positivity of the consistency, power-law indices and densities. For example, in [14] a simple linear mixture law was used for simplicity. It's clear from proposition 3 and

lemma 1, that we require $m = \sup_\Omega\{m\}$. Similarly, in the interface-tracking formulation, we take $m = \max_k\{m_k\}$. Physically, this corresponds to the fluid that has the smallest power law index, *i.e.*, is shear thinning to the greatest extent.

Remark 2: For displacements involving shear thinning fluids, $n < 1$, we have that $m > 1$ and hence $W^{1,1+1/m}(\Omega) \not\subset H^1(\Omega)$, whereas for shear-thickening displacements and those involving Bingham fluids, $n \geq 1$, and due to the Sobolev embedding theorems we have $\Psi \in W^{1,1+1/m}(\Omega) \subset H^1(\Omega)$.

Remark 3: For the reader unfamiliar with this formalism and terminology, very loosely speaking, $L^2(\Omega)$ is the space of functions that are defined almost everywhere and whose square is integrable over the two-dimensional domain Ω. Similarly, $W^{1,1+1/m}(\Omega)$ is a space of functions with partial derivatives defined almost everywhere and for which the $(1 + 1/m)$-th power of the absolute value of the gradient is integrable over Ω. Thus we have shown that if, the data for (7) is square-integrable, we can always find a stream function that is differentiable almost everywhere and that satisfies (37). This function is regarded as a *weak* solution to (7) in that for the classical formulation (7), we would require also that second derivatives are defined.

4. Steady-state displacements

The existence and uniqueness results are very general, covering a wide range of geometries as would typically be found in a well. We now address the question of whether a steady-state, (travelling wave), solution can be found. For this we shall consider the interface-tracking formulation, both for simplicity and since we will seek an analytical form for the shape of the steady interface. From a physical perspective, such solutions are to be expected in certain situations, *e.g.* a heavier more viscous fluid slowly displacing a lighter less viscous fluid upwards in a vertical concentric annulus.

Since the mean axial speed at a depth ξ in the well is given by $Q(t)/[\bar{H}(\xi)r_a(\xi)]$, it is apparent that a steady-displacement solution cannot exist if the geometry is changing along the length of the well. Additionally, $Q(t)$ enters only through the boundary conditions. Therefore, we assume that the well is uniform in the ξ-direction and that a constant flow rate is pumped. Without loss of generality, the scalings in [14] give that: $\bar{H} = r_a = 1$ and we may assume $Q(t) = 1$. We also assume that $\beta(\xi)$ and $e(\xi)$ are constant. This situation is not wholly unrealistic in considering a well, since typically $Z \gg 1$, whereas the slowly changing axial geometry changes on an intermediate length-scale, L:

$$1 \ll L \ll Z,$$

e.g. L could be related to the length of a stand of casing, the separation between centralisers, or radius of curvature of the drilled hole, all of which are much longer than the circumference, which has been used as the length-scale, (*i.e.*, this ignores $O(1)$ changes in annular geometry, such as washouts, which in any case violate the model assumptions). Secondly, for laboratory-based experimental studies, it is easiest to construct a uniform annulus.

For the interface-tracking formulation, we consider only two fluids and introduce a frame of reference (z, ϕ) where $z = \xi - t$ is moving with the mean speed of the flow, (= unity). The interface separates fluid 1, the lower displacing fluid, from the displaced fluid 2. We consider a long domain $z \in (-L, L)$, with the steady interface centred at $z = 0$. We denote the interface position in the moving frame by:

$$z = g(\phi, t) = h(\phi, t) - t, \tag{53}$$

and write the stream function Ψ as

$$\Psi = \Phi + \phi + \frac{e}{\pi}\sin\pi\phi, \tag{54}$$

i.e., Φ is the stream function in the moving frame. The kinematic equation (18) becomes

$$(1 + e\cos\pi\phi)\frac{\partial g}{\partial t} - \frac{\partial\Phi}{\partial z}\frac{\partial g}{\partial\phi} = \frac{\partial\Phi}{\partial\phi}, \tag{55}$$

The field equations for Φ in the moving frame are (16) and (17), in lower and upper domains, respectively, with constitutive laws (8) and (9). Boundary conditions for Φ are:

$$\Phi(0, z) = \Phi(1, z) = 0, \tag{56}$$

c.f. conditions (12) and (13), and

$$\frac{\partial\Phi}{\partial z}(\phi, \pm L) = 0, \tag{57}$$

i.e., our section of the annulus is somewhere away from the ends, ($\xi = 0,\ Z$), and once we move away from the interface a sufficiently large distance, L, the annulus is filled with a single fluid, flowing parallel to the axis of the annulus. At the interface the following two continuity conditions are satisfied,

$$[\Phi]_1^2 = 0, \tag{8}$$

$$\left[\frac{\rho_k\cos\beta}{\mathrm{St}^*}\frac{\partial g}{\partial\phi} - \frac{\rho_k\sin\beta\sin\pi\phi}{\mathrm{St}^*}\right]_1^2 = \left[\left(\frac{\chi_k + \dfrac{\tau_{k,Y}}{H}}{|\nabla(\Phi + \phi + \dfrac{e}{\pi}\sin\pi\phi)|}\right)\times \left(\frac{\partial\Phi}{\partial z} - [\frac{\partial\Phi}{\partial\phi} + 1 + e\cos\pi\phi]\frac{\partial g}{\partial\phi}\right)\right]_1^2 \tag{59}$$

c.f. conditions (20) and (23). Note that for a steady state displacement, both fluids must be yielded at the interface.

In general we will seek steady g and Φ. If g is steady, then (55) corresponds to saying that the interface is a streamline, (*i.e.*, for Φ). Since the interface must intercept $\phi = 0$ and $\phi = 1$, where (56) is satisfied, it follows that $\Phi = 0$ on a steady interface. In the following situations we are able to find an analytical solution for both g and Φ.

4.1. Concentric annuli: $e = 0$

This is certainly the simplest case possible and one in which, at least when vertical, our intuition tells us that there must exist a steady state.

Setting $\Phi = 0$ gives that $\Psi = \phi$. Hence $\nabla\Psi = (1, 0)$, and since $\boldsymbol{S}_k$ is constant in fluid k, the field equations (16) and (17) are both satisfied. It remains only to satisfy (59), which simplifies to:

$$\left[\chi_k(1) + \tau_{k,Y} + \frac{\rho_k\cos\beta}{\mathrm{St}^*}\right]_1^2\frac{\partial g}{\partial\phi} = \left[\frac{\rho_k\sin\beta}{\mathrm{St}^*}\right]_1^2\sin(\pi\phi), \tag{60}$$

which gives the shape of the interface up to an additive constant, (set to zero):

$$g(\phi) = -\frac{1}{\pi}\frac{b\sin\beta}{\left[\chi_k(1)+\tau_{k,Y}\right]_1^2 + b\cos\beta}\cos\pi\phi, \tag{61}$$

where b is the buoyancy parameter:

$$b = \frac{\rho_2 - \rho_1}{\mathrm{St}^*}, \tag{62}$$

which will typically be negative since a more dense fluid is usually used to displace a lighter one. Although simplistic, this solution gives a number of insights.

1. The term $(\chi_k(1)+\tau_{k,Y})$ is the pressure gradient in each fluid, which is in the axial direction only. Thus, the fraction in (61) represents the ratio of differences in the azimuthal and axial modified pressure gradients. If the jump in modified pressure gradients is predominantly axial, the steady state will be *flat*, whereas if the jump is predominantly azimuthal the steady state will elongate along axis of the well. Thus, for a fixed density difference, increasing the frictional pressure drop in the displacing fluid, *i.e.*, $(\chi_1(1)+\tau_{1,Y})$, will tend to flatten the steady-state profile.
2. Vertical well: Here $\beta = 0$ giving $g(\phi) =$ constant, *i.e.*, the steady-state interface is horizontal as expected.
3. Inclined well: With no rheology difference, we have simply

$$g(\phi) = -\frac{1}{\pi}\tan\beta\cos\pi\phi, \tag{63}$$

   which implies that the interface aligns perpendicular to the direction of gravity. Note also that in cementing, the Stokes number St^* is typically small, so that relatively small density differences can lead to large buoyancy b. The above shape is that approached in the limit $b \to \infty$, and is independent of the density difference.
4. Horizontal well: Here $\beta = \pi/2$ and we obtain:

$$g(\phi) = -\frac{1}{\pi}\frac{b}{\left[\chi_k(1)+\tau_{k,Y}\right]_1^2}\cos(\pi\phi). \tag{64}$$

   In a horizontal well there will naturally be a tendency for the heavier fluid to slump towards the bottom of the annulus. Equation (64) is interesting in that it indicates that these buoyancy effects can be compensated by rheological effects, resulting in a steady state.

Various examples of the variations in (61) are shown in Section 4.4.

4.2. Mildly eccentric annuli: $e \ll 1$

In this section, we show that it is also possible to derive an analytical solution in the case that $e \ll 1$, by means of a regular perturbation expansion.

In applying this method we linearise with respect to e, not only about the zeroth order solution, but also about the zeroth order domain, *i.e.*, steady-state shape. Since we wish to find an analytical solution, via separation of variables, we require that the zeroth order domain shape be rectangular, meaning that we must impose the requirement that the zeroth order

steady state shape is of $O(e)$, (*i.e.*, the fully concentric solution g, derived in the above section, is small). This requirement is equivalent to assuming that

$$\frac{b\sin\beta}{\left[\chi_k(1,1)+\tau_{k,Y}\right]_1^2+b\cos\beta}\sin\pi\phi = O(e). \tag{65}$$

Condition (65) is likely to be satisfied either in a nearly-vertical well, $\beta \ll 1$, or if the frictional pressure difference is much greater than the buoyancy parameter. Thus, our results will be slightly restrictive. However, in including eccentricity they will still give good insight into the effects of parameter variations on steady state shape.

We seek regular perturbation solutions of form:

$$\Phi(z,\phi) = e\Phi_1(z,\phi) + e^2\Phi_2(z,\phi) + \ldots \qquad g(\phi) = eg_1(\phi) + e^2 g_2(\phi) + \ldots$$

with

$$\Psi = \Phi + (\phi + \frac{e}{\pi}\sin\pi\phi),$$

and $H = 1 + e\cos\pi\phi$. We substitute these expressions in (16) and (17) and into the rheological laws (8) and (9), expand with respect to small e and retain only the $O(e)$ terms, giving:

$$(\chi_k'(1,1) + \chi_{k,H}(1,1) - \tau_{k,Y})\pi\sin\pi\phi = (\chi_k(1,1)+\tau_{k,Y})\frac{\partial^2\Phi_1}{\partial z^2} + \chi_k'(1,1)\frac{\partial^2\Phi_1}{\partial\phi^2} \tag{66}$$

in each of the fluid domains Ω_k; $k = 1, 2$. Note that we now denote $\chi_k = \chi_k(|\nabla_a\Psi|, H)$, since we have linearised both with respect to the solution Φ and with respect to the geometry H. To leading order, our zeroth order solution has $(|\nabla_a\Psi|, H) = (1, 1)$. We denote by χ_k' the partial derivative of χ_k with respect to $|\nabla_a\Psi|$, and by $\chi_{k,H}$, the partial derivative of χ_k with respect to H.

Equation (66) is a linear elliptic equation in Ω_k. Assuming (65), we may linearise the domains, giving to leading order: $\Omega_1 = (0,1)\times(-L,0)$ and $\Omega_2 = (0,1)\times(0,L)$. Boundary conditions at $\phi = 0, 1$ for the two domains are (56) and at $z = \pm L$ we have (57). The zeroth order interface is the line $z = 0$, along which (58) and (55) imply that

$$\Phi(\phi, 0) = 0, \tag{57}$$

see our earlier discussion. These boundary conditions are sufficient to calculate the solution Φ_1 to (66) in each domain, (*e.g.* by homogenizing (66) and using separation of variables). The analytical solutions are:

$$\Phi_1(\phi,z) = \left(1 + \frac{\chi_{1,H}(1,1)-\tau_{1,Y}}{\chi_1'(1,1)}\right)\left(-1+\frac{\cosh\alpha_1(L+z)}{\cosh\alpha_1 L}\right)\frac{\sin\pi\phi}{\pi}, \qquad (\phi,z)\in\Omega_1, \tag{68}$$

$$\Phi_1(\phi,z) = \left(1 + \frac{\chi_{2,H}(1,1)-\tau_{2,Y}}{\chi_2'(1,1)}\right)\left(-1+\frac{\cosh\alpha_2(L-z)}{\cosh\alpha_2 L}\right)\frac{\sin\pi\phi}{\pi}, \qquad (\phi,z)\in\Omega_2, \tag{69}$$

where

$$\alpha_k^2 = \frac{\pi^2 \chi_k'(1,1)}{\chi_k(1,1)+\tau_{k,Y}} > 0. \tag{70}$$

To determine the shape of the interface, we linearise (59), to give:

$$\begin{aligned} 0 = \; & e\left[(\chi_k(1,1)+\tau_{k,Y})(\frac{\partial \Phi_1}{\partial z}(\phi,0) - \frac{\partial g_1}{\partial \phi}) - \frac{\rho_k \cos\beta}{\mathrm{St}^*}\frac{\partial g_1}{\partial \phi}\right]_1^2 \\ & + \left[\frac{\rho_k \sin\beta \sin\pi\phi}{\mathrm{St}^*}\right]_1^2 + O(e^2). \end{aligned} \tag{71}$$

Note that, because of (65), both terms above have the same order. Rearranging we have:

$$\frac{\partial g_1}{\partial \phi} = \frac{1}{e}\frac{b\sin\beta}{\left[\chi_k(1,1)+\tau_{k,Y}\right]_1^2 + b\cos\beta}\sin\pi\phi + \frac{\left[(\chi_k(1,1)+\tau_{k,Y})\dfrac{\partial \Phi_1}{\partial z}(\phi,0)\right]_1^2}{\left[\chi_k(1,1)+\tau_{k,Y}\right]_1^2 + b\cos\beta}. \tag{72}$$

The first term above is simply the concentric annular solution. The second term represents the effect of eccentricity.

To simplify matters, we note that, on using (5) and straightforward algebra:

$$\chi_H(1,1) - \tau_Y = -\frac{\chi'(1,1)\chi^m(1,1)}{\kappa^m}, \tag{73}$$

and that

$$1 - \frac{\chi'(1,1)\chi^m(1,1)}{\kappa^m} = -P(\chi(1,1),\tau_Y,m), \tag{74}$$

where $P(\chi(1,1),\tau_Y,m)$ is the strictly positive function given by:

$$P(\chi,\tau_Y,m) = \frac{(m+1)^2\chi^2 + (m+2)(2m+1)\chi\tau_Y + (m+1)(m+2)\tau_Y^2}{\chi[(m+1)\chi + (m+2)\tau_Y]}. \tag{75}$$

We use (73–75), substitute for Φ_1, simplify and integrate to give the interface position:

$$\begin{aligned} g(\phi) \sim \; & -\frac{1}{\pi}\frac{b\sin\beta}{\left[\chi_k(1,1)+\tau_{k,Y}\right]_1^2 + b\cos\beta}\cos\pi\phi \\ & -\frac{e}{\pi^2}\frac{\displaystyle\sum_{k=1,2} P(\chi_k,\tau_{k,Y},m_k)(\chi_k+\tau_{k,Y})\alpha_k \tanh\alpha_k L}{\left[\chi_k(1,1)+\tau_{k,Y}\right]_1^2 + b\cos\beta}\cos\pi\phi, \end{aligned} \tag{76}$$

i.e., subject to (65). The simplified solution for Φ is

$$\Phi(\phi,z) \sim eP(\chi_1(1,1),\tau_{1,Y},m_1)\left(1 - \frac{\cosh\alpha_1(L+z)}{\cosh\alpha_1 L}\right)\frac{\sin\pi\phi}{\pi} + O(e^2), \quad (\phi,z)\in\Omega_1, \tag{77}$$

$$\Phi(\phi,z) \sim eP(\chi_2(1,1),\tau_{2,Y},m_2)\left(1 - \frac{\cosh\alpha_2(L-z)}{\cosh\alpha_2 L}\right)\frac{\sin\pi\phi}{\pi} + O(e^2), \quad (\phi,z)\in\Omega_2. \tag{78}$$

4.3. REMARKS

The asymptotic solutions for the interface (76) and the stream function in each domain (77) and (78) are interesting primarily because all the problem parameters appear in the solutions, (eccentricity, inclination, density difference, fluid rheologies). Although we require that (65) be satisfied and that $e \ll 1$, in order to get quantitatively accurate results, the methodology does not necessarily break down if (65) is not satisfied. Thus, we may consider that the parametric trends remain qualitatively correct at least partly outside of the strict domain of validity or our approximation. To justify this statement, note that if we relax (65) and thus assume

$$\Phi(z,\phi) = e\Phi_1(z,\phi) + e^2\Phi_2(z,\phi) + \ldots \qquad g(\phi) = g_0(\phi) + eg_1(\phi) + e^2 g_2(\phi) + \ldots$$

this has no effect on (66), *i.e.*, we still solve a linear Poisson equation in Ω_1 and Ω_2. Unfortunately the domains are now:

$$\Omega_1 = (0,1) \times (-L, g_0(\phi)), \qquad \Omega_2 = (0,1) \times (g_0(\phi), L).$$

This makes analytical solution difficult, but a numerical solution could be fairly easily obtained. The difference now comes in the linearisation of (59). In place of (71), the zeroth and first order terms are:

$$\frac{\partial g_0}{\partial \phi} = \frac{b \sin\beta}{\left[\chi_k(1,1) + \tau_{k,Y}\right]_1^2 + b\cos\beta} \sin\pi\phi, \tag{79}$$

$$\begin{aligned}\frac{\partial g_1}{\partial \phi} = {} & \frac{\left[(\chi_k(1,1) + \tau_{k,Y})\dfrac{\partial \Phi_1}{\partial z}(\phi, g_0) - \chi_k'(1,1)\dfrac{\partial \Phi_1}{\partial \phi}(\phi, g_0)\right]_1^2}{\left[\chi_k(1,1) + \tau_{k,Y}\right]_1^2 + b\cos\beta} \\ & + \frac{\left[(\tau_{k,Y} - \chi_k'(1,1) - \chi_{H,k}(1,1))\cos\pi\phi \dfrac{\partial g_0}{\partial \phi}\right]_1^2}{\left[\chi_k(1,1) + \tau_{k,Y}\right]_1^2 + b\cos\beta}.\end{aligned} \tag{80}$$

The zeroth order term is instantly recognisable as (61). The first-order term is much more complex than (71). From (80) we can see that higher harmonics will start to appear in our perturbation solution, as is usual. Although numerical solution of (66) and the complexity in (80) prohibit continuing, there is no indication that the perturbation method itself breaks down.

In (76) we can observe the effect of eccentricity on the concentric solution. The numerator of the second term is strictly positive. Intuition tells us that the displacing fluid should be heavier and more *viscous* than the displaced fluid. In this case, the denominator of the second term is negative and we see that the second term in (76) is of form $e \times C \times \cos\pi\phi$, for some $C > 0$. Thus, in a near vertical well, (so that (65) is valid), for positive density and frictional pressure differences, (as advocated for such field operations, see [10]), the effect of eccentricity is to compensate for the first term in (76) by extending the steady-state interface upwards along the wide side.

Much of the algebraic complexity in our solutions is due to the fluids having a yield stress. When there is no yield stress present, explict formulas can be derived for most of the parameters; (76–78) become:

$$g(\phi,z)\sim -\frac{1}{\pi}\frac{b\sin\beta}{\left[\kappa_k(m_k+1)^{1/m_k}\right]_1^2+b\cos\beta}\cos\pi\phi \\ -\frac{e}{\pi}\frac{\sum_{k=1,2}\kappa_k(m_k+1)^{1+1/m_k}m_k^{-1/2}\tanh(\pi m_k^{-1/2}L)}{\left[\kappa_k(m_k+1)^{1/m_k}+\right]_1^2+b\cos\beta}\cos\pi\phi. \tag{81}$$

$$\Phi(\phi,z)\sim e(m_1+1)\left(1-\frac{\cosh\pi m_1^{-1/2}(L+z)}{\cosh\pi m_1^{-1/2}L}\right)\frac{\sin\pi\phi}{\pi}+O(e^2),\ (\phi,z)\in\Omega_1, \tag{82}$$

$$\Phi(\phi,z)\sim e(m_2+1)\left(1-\frac{\cosh\pi m_2^{-1/2}(L-z)}{\cosh\pi m_2^{-1/2}L}\right)\frac{\sin\pi\phi}{\pi}+O(e^2),\ (\phi,z)\in\Omega_2. \tag{83}$$

These expressions are valid for power-law fluids, (and Newtonian fluids, $m=1$).

Finally, we may consider what happens in the far-field. For the stream function we may set $z=\mp L$ in (77) and (78), respectively. At large L the terms divided by $\cosh\alpha_k L$ may be neglected, (formally $L\to\infty$), leaving simply the far field stream functions, which we write as $\Phi_{\mp\infty}(\phi)$, given by:

$$\Phi_{-\infty}(\phi)=eP(\chi_1,\tau_{1,Y},m_1)\frac{\sin\pi\phi}{\pi};\qquad \Phi_{\infty}(\phi)=eP(\chi_2,\tau_{2,Y},m_2)\frac{\sin\pi\phi}{\pi}. \tag{84, 85}$$

The far-field velocities $\overline{w}_{\mp\infty}(\phi)$ on the wide ($\phi=0$) and narrow ($\phi=1$) sides of the annulus (in the original frame of reference) are:

$$\overline{w}_{-\infty}(0)\sim 1+eP(\chi_1,\tau_{1,Y},m_1);\qquad \overline{w}_{-\infty}(1)\sim 1-eP(\chi_1,\tau_{1,Y},m_1), \tag{86, 87}$$

$$\overline{w}_{\infty}(0)\sim 1+eP(\chi_2,\tau_{2,Y},m_2);\qquad \overline{w}_{\infty}(0)\sim 1-eP(\chi_2,\tau_{2,Y},m_2). \tag{88, 89}$$

Thus, the function $P(\chi(1,1),\tau_Y,m)$ measures the maximal velocity differential between the far-field and the steady state. In the case of a power law fluid, we have:

$$P(\chi,\tau_Y,m)=m+1,$$

and the velocity differential is clearly larger for large m, *i.e.*, for shear-thinning fluids, as is intuitive. It is interesting to note that in this case the velocity differential depends only on the power-law index and not on the consistency of each fluid. For a Newtonian fluid, the ratio of wide to narrow side velocities is simply: $(1+2e)/(1-2e)$.

4.4. Illustrative results

In Figure 4 we plot three examples of the stream-function solution in the moving frame, (77) and (78). Note that our solution is independent of buoyancy and inclination. In Figure 4a the displacing fluid has significantly higher yield stress, consistency and power law index $(1/m)$, than the displaced fluid. The streamlines are more densely packed in the *less viscous* upper fluid, indicating that the effects of eccentricity are felt more acutely here. In Figure 4b the eccentricity has been reduced, giving a consequent (linear in e) reduction in the velocity perturbation. Finally, in Figure 4c we increase the yield stress consistency and power-law

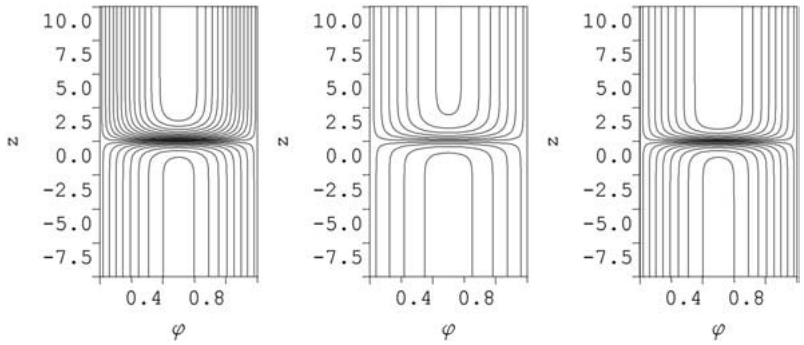

Figure 4. The function Φ, for parameters $L = 10$, $\tau_{1,Y} = \kappa_1 = m_1 = 1{\cdot}0$: (left to right) a) $e = 0{\cdot}1$, $\tau_{2,Y} = 0{\cdot}5$, $\kappa_2 = 0{\cdot}5$, $m_2 = 2{\cdot}0$; b) $e = 0{\cdot}05$, $\tau_{2,Y} = 0{\cdot}5$, $\kappa_2 = 0{\cdot}5$, $m_2 = 2{\cdot}0$; c) $e = 0{\cdot}1$, $\tau_{2,Y} = 0{\cdot}9$, $\kappa_2 = 0{\cdot}9$, $m_2 = 1{\cdot}1$. Streamlines are spaced at intervals $\Delta\Phi = 0{\cdot}01$.

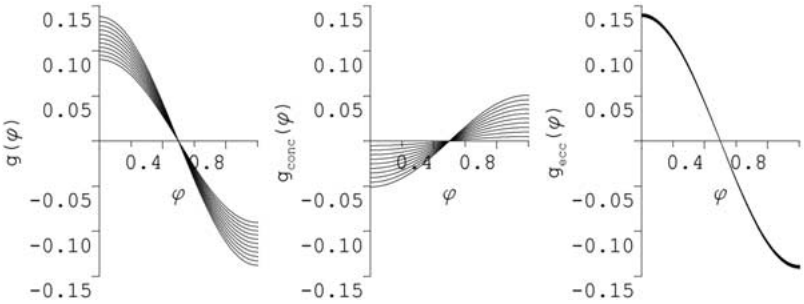

Figure 5. Parametric variations in $g(\phi)$, $g_{\mathrm{conc}}(\phi)$ and $g_{\mathrm{ecc}}(\phi)$ with inclination β: $\beta = 0, 0{\cdot}03, 0{\cdot}06, \ldots, 0{\cdot}3$; $g_{<rmconc}(\phi)$ elongates negatively, $g_{\mathrm{ecc}}(\phi)$ elongates positively. Fixed parameters are: $e = 0{\cdot}05$, $b = -1$, $\tau_{1,Y} = 1$, $\kappa_1 = 1$, $m_1 = 1$, $\tau_{2,Y} = 0{\cdot}8$, $\kappa_2 = 0{\cdot}8$, $m_2 = 1{\cdot}0$.

index of the displaced fluid, to close to that of fluid 1. The streamlines in the two domains are quite similar.

In Figures 5–10 we explore the variations in (76) with the model parameters. We fix a base case for the parameters: $\beta = 0{\cdot}1$, $e = 0{\cdot}05$, $b = -1$, $\tau_{1,Y} = 1$, $\kappa_1 = 1$, $m_1 = 1$, $\tau_{2,Y} = 0{\cdot}8$, $\kappa_2 = 0{\cdot}8$, $m_2 = 1{\cdot}0$, and for each of Figures 5–10 we vary just one parameter to explore the sensitivity. For the rheological parameters, for brevity, we show only the results of varying the properties of fluid 2; qualitatively similar effects are achieved by changing fluid 1 properties in the opposite direction to fluid 2 parameters.

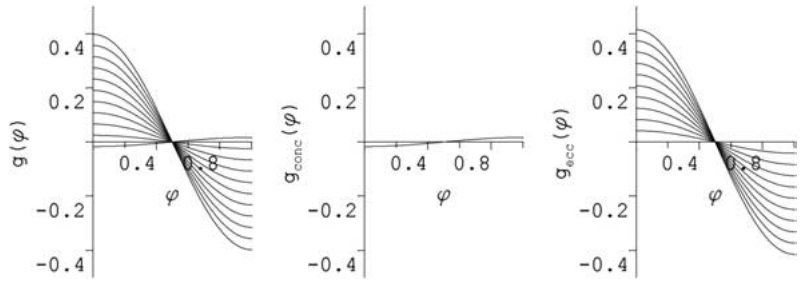

Figure 6. Parametric variations in $g(\phi)$, $g_{\mathrm{conc}}(\phi)$ and $g_{\mathrm{ecc}}(\phi)$ with eccentricity e: $e = 0, 0{\cdot}015, 0{\cdot}03, \ldots, 0{\cdot}15$; $g_{\mathrm{conc}}(\phi)$ is unaffected, $g_{\mathrm{ecc}}(\phi)$ elongates positively. Fixed parameters are $\beta = 0{\cdot}1$, $b = -1$, $\tau_{1,Y} = 1$, $\kappa_1 = 1$, $m_1 = 1$, $\tau_{2,Y} = 0{\cdot}8$, $\kappa_2 = 0{\cdot}8$, $m_2 = 1{\cdot}0$.

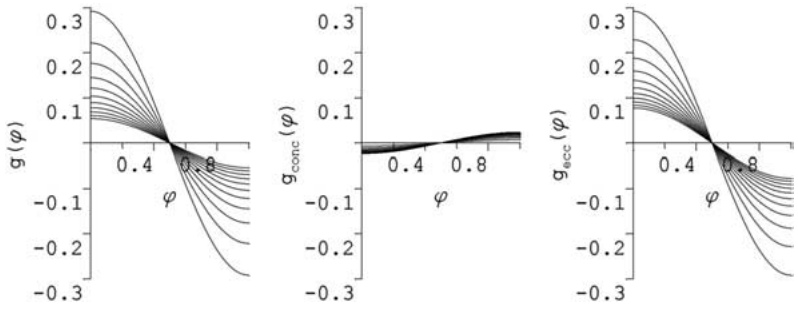

Figure 7. Parametric variations in $g(\phi)$, $g_{\text{conc}}(\phi)$ and $g_{\text{ecc}}(\phi)$ with buoyancy b: $b = 0, -0{\cdot}25, -0{\cdot}5, \ldots, -2{\cdot}5$; $g_{\text{conc}}(\phi)$ elongates negatively, $g_{\text{ecc}}(\phi)$ flattens. Fixed parameters are $\beta = 0{\cdot}1$, $e = 0{\cdot}05$, $\tau_{1,Y} = 1$, $\kappa_1 = 1$, $m_1 = 1$, $\tau_{2,Y} = 0{\cdot}8$, $\kappa_2 = 0{\cdot}8$, $m_2 = 1{\cdot}0$.

In each of Figures 5–10 we plot $g(\phi)$ from (76), and also the functions $g_{\text{conc}}(\phi)$ and $g_{\text{ecc}}(\phi)$. The function $g_{\text{conc}}(\phi)$ is the concentric annular solution (61), also the first term in (76). The function $g_{\text{ecc}}(\phi)$ is the second term in (76), which contains all the effects of eccentricity. Thus, we compare the effects of each parameter on both the concentric and eccentric terms in (76).

Since our model has assumed (65) to hold, the variations in $g_{\text{conc}}(\phi)$ in Figures 5–10 are typically smaller than those in $g_{\text{ecc}}(\phi)$. Often the observed effects are contrary between $g_{\text{conc}}(\phi)$ and $g_{\text{ecc}}(\phi)$, and due to (65) the eccentric effects dominate. Although eccentricity is certainly an important parameter, one should not conclude that it is always dominant. A better way of interpreting our results is as a competition between $g_{\text{conc}}(\phi)$ and $g_{\text{ecc}}(\phi)$, *i.e.*, specifically, $g_{\text{ecc}}(\phi)$ is a perturbation of $g_{\text{conc}}(\phi)$. The relevant feature is usually whether or not increasing a parameter serves to elongate or flatten the steady-state profile. These qualitative effects are summarised below.

- $g_{\text{conc}}(\phi)$ is elongated negatively, (*i.e.*, $g_{\text{conc}}(0) - g_{\text{conc}}(1) < 0$ and $|g_{\text{conc}}(0) - g_{\text{conc}}(1)|$ increases), by the following variations: increasing β, $\tau_{2,Y}$, κ_2, $n_2 = 1/m_2$; decreasing b, $\tau_{1,Y}$, κ_1, $n_1 = 1/m_1$.
- $g_{\text{ecc}}(\phi)$ is elongated positively, (*i.e.*, $g_{\text{ecc}}(0) - g_{\text{ecc}}(1) > 0$ and $|g_{\text{ecc}}(0) - g_{\text{ecc}}(1)|$ increases), by the following variations: increasing β, b, e, $\tau_{2,Y}$, κ_2, $n_2 = 1/m_2$; decreasing $\tau_{1,Y}$, κ_1, $n_1 = 1/m_1$.

In making the above statements, it must be noted that we have explored *small* parametric variations about a set of parameters that might be thought *sensible* to achieve a steady-state displacement, *i.e.*, we ensure a hierarchy in both the rheological parameters and densities of the 2 fluids, (heavy and viscous displaces light and less viscous). Inspection of the denominator of the two terms in (76) shows that these solutions can become singular if we consider for example a negative rheology difference *vs.* a positive density difference. Such solutions are not explored here.

5. Discussion and conclusions

This paper has addressed the issue of whether steady-state displacements can exist during primary cementing of an oil well. Two questions have been answered affirmatively. Firstly, in Section 3 we have shown that for more or less any physically sensible distribution of fluid concentrations or fluid interfaces, (*i.e.*, depending on the preferred model formulation), there exists a unique stream function. Obviously, this is a necessary condition to finding any steady

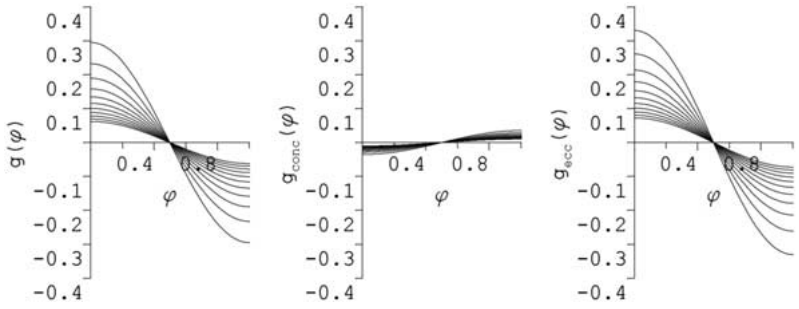

Figure 8. Parametric variations in $g(\phi)$, $g_{\text{conc}}(\phi)$ and $g_{\text{ecc}}(\phi)$ with displaced fluid yield stress $\tau_{2,Y}$: $\tau_{2,Y} = 0, 0{\cdot}15, 0{\cdot}3, \ldots, 1{\cdot}5$; $g_{\text{conc}}(\phi)$ elongates negatively, $g_{\text{ecc}}(\phi)$ elongates positively. Fixed parameters are $\beta = 0{\cdot}1$, $e = 0{\cdot}05$, $b = -1$, $\tau_{1,Y} = 1$, $\kappa_1 = 1$, $m_1 = 1$, $\kappa_2 = 0{\cdot}8$, $m_2 = 1{\cdot}0$.

solution. Secondly, in Section 4 we have derived explicit analytic expressions for steady-state solutions.

The existence results, although only for a weak solution, are really very comprehensive in terms of likely situations to be encountered in modelling primary cementing. In effect they ensure, from a theoretical standpoint, that the model derived in [14] is mathematically sensible. Physical sensibility of this same model is addressed in [14], where the derivation is careful. Although we have not done so here, it appears possible to derive various results relating to well-posedness of the problem for Ψ, by considering this variational formulation. A second issue, that we have partly addressed and which will be presented in a subsequent work, [34], is the question of accurate numerical solution for Ψ.

Turning to the results in Section 4, which have already been explored and discussed in some depth, these analytical solutions serve a number of important purposes. First, they confirm unequivocally that steady-state displacements can exist in primary cementing. Second, they allow quick comparison with our physical intuition. In particular this is true for the concentric annular solutions. Third, the solutions give a direct quantitative indication of how large competing effects of different parameters are, at least within the range of validity. For example, one might estimate the rheology difference required to counter slumping effects in a horizontal displacement. Fourth, the solutions provide a test case for numerical solutions. We note here that for certain simple cases, (*e.g.* two fluids displacing in a uniform annulus with no intermediate concentrations), a formal equivalence can be established between the interface tracking and fluid mixture formulations.

Despite of the usefulness of Section 4, the results are in a sense incomplete in that we have not considered the question of stability. It is evident in (61) that if we interchange the fluid properties between fluids 1 and 2, we will leave the shape of steady state unchanged! Certainly, some of these configurations (*e.g.* a light fluid displacing a heavy fluid, with identical rheology) are simply mechanically unstable, and would not be observed in reality. The question of whether there exist stable steady states is harder to answer, although numerical results shown in [14] do suggest that this is the case. Pragmatically, we may assume that some steady states will be stable, others not. In a subsequent paper, [34], we begin to address some of these questions of stability.

In the situation of a vertical concentric annulus, one might improve one's understanding of stability. This situation corresponds to a planar displacement along the axis of the annulus. Similarly, an approximately planar displacement can be achieved for certain small e solutions,

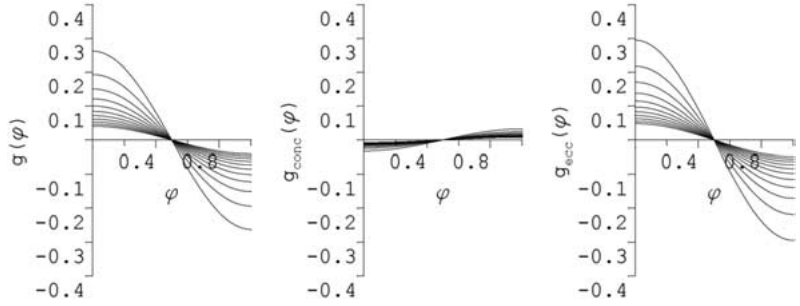

Figure 9. Parametric variations in $g(\phi)$, $g_{\mathrm{conc}}(\phi)$ and $g_{\mathrm{ecc}}(\phi)$ with displaced fluid consistency κ_2: $\kappa_2 = 0{\cdot}1, 0{\cdot}2, 0{\cdot}3, \ldots, 1{\cdot}1$; $g_{\mathrm{conc}}(\phi)$ elongates negatively, $g_{\mathrm{ecc}}(\phi)$ elongates positively. Fixed parameters are $\beta = 0{\cdot}1$, $e = 0{\cdot}05$, $b = -1$, $\tau_{1,Y} = 1$, $\kappa_1 = 1$, $m_1 = 1$, $\tau_{2,Y} = 0{\cdot}8$, $m_2 = 1{\cdot}0$.

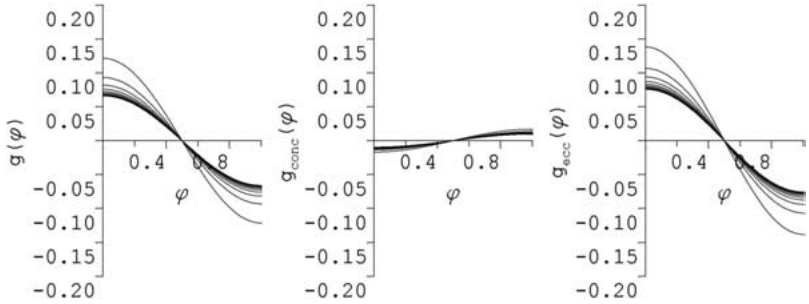

Figure 10. Parametric variations in $g(\phi)$, $g_{\mathrm{conc}}(\phi)$ and $g_{\mathrm{ecc}}(\phi)$ with displaced fluid inverse-power-law index m_2: $m_2 = 1{\cdot}0, 1{\cdot}3, 1{\cdot}6, \ldots, 4{\cdot}0$; $g_{\mathrm{conc}}(\phi)$ flattens, $g_{\mathrm{ecc}}(\phi)$ flattens. Fixed parameters are $\beta = 0{\cdot}1$, $e = 0{\cdot}05$, $b = -1$, $\tau_{1,Y} = 1$, $\kappa_1 = 1$, $m_1 = 1$, $\tau_{2,Y} = 0{\cdot}8$, $\kappa_2 = 0{\cdot}8$.

where $g_{\mathrm{conc}}(\phi)$ and $g_{\mathrm{ecc}}(\phi)$ approximately balance each other. Local stability analyses of this type of flow have been carried out in [24–26], in the context of a porous media displacement of non-Newtonian fluids. Recently also stability of planar displacement of a Herschel-Bulkley fluid in a Hele-Shaw cell, (*i.e.*, the Saffman-Taylor problem), has been partly addressed in [29]; see also the discussion in [27]. Although partly relevant, it must be noted that this type of analysis is local and is focused at instability, meaning the local viscous fingering of the interface. In the context of primary cementing of an oil well, where $Z \gg 1$, it is the global behaviour of an instability that is of concern. More specifically, the relevant question is whether or not a displacement results in an unwanted flow structure that extends a significant length along the well. Any 'defect' that affects only an axial length of $O(1)$ is unlikely to compromise the hydraulic isolation of the cement job. In a subsequent paper we will address the prediction of such global defects.

Acknowledgements

This research has been carried out at the University of British Columbia, supported financially by Schlumberger and NSERC through CRD project 245434, as well as by the Pacific Institute for the Mathematical Sciences. This support is gratefully acknowledged. We thank the referees for their helpful comments.

Notes

[1]In choosing a Herschel-Bulkley model we acknowledge that we are making a modelling idealisation, and this is discussed further in [14]. Drilling muds, spacer fluids and cement slurries are in fact suspensions, and are quite complex in both their composition and rheological properties. For the modelling of cementing displacements the key features that need to be represented are the shear-thinning behaviour and the yield stress. We consider the fluids to be inelastic, although visco-elasticity can be important in certain situations and for certain wellbore fluids. Additionally, if static, a gel-strength generally builds up. The point is that there is not a generic drilling mud, spacer or cement slurry. Indeed many oilfield companies derive their competitive advantage by the chemical design of these fluids with specific rheological properties. When flowing, both drilling muds and cement slurries are predominantly shear thinning, nonlinearly viscous and inelastic, often with a significant yield stress. This is signified by the fact that rheological models such as the Bingham or power-law model are frequently used in the industry to characterise these fluids. Hence, the Herschel-Bulkley model is relevant as a more comprehensive model incorporating current industry practice.

We also point out that there can be significant problems in assigning (*i.e.*, measuring) values for parameters such as the yield stress, (and hence also the consistency and power-law index). Part of these problems are concerned with the fact that an ideal yield stress fluid, whilst mathematically consistent, does not fully represent reality. In fact, below the *yield stress* fluids might exhibit linear elastic behaviour, or slow creep, or be very very viscous, or some combination of these. There has been a long-standing debate, (which need not be revived here), in rheological circles concerning the precise nature of the yield stress. A second problem concerns measurement techniques, which are not always found to be scale-invariant. This can be particularly true with suspensions, for which a range of phenomena can occur, (*e.g.*, sedimentation, slip at the walls, etc.). Although here the annular gap in which the displacement flow occurs is of the order of a centimeter, it is worth remarking that in porous media (with which we have a strong analogy) the micro-scale of the porous media and fluid suspension can often be comparable. Objectively, this means that the limiting pressure gradients and other rheological characteristics cease to be simply a function of the fluid. This can make the strictly mathematical approach to porous media modelling, in which one essentially homogenizes the flow through an appropriate tube-bundle, either invalid or at most a conceptual aid. All of these topics, although important, are beyond the scope of this paper.

[2]Note that a suitable Ψ^* can be defined by taking a linear combination of stream functions at $\xi = 0$ and $\xi = Z$. So in case of two fluids we can take $\Psi^* = (1 - c)\Psi_0 + c\Psi_Z$, where Ψ_a is the stream function at $\xi = a$, see (14) and (15) and c is the concentration with $c = 0$ for the displacing fluid and $c = 1$ for the displaced fluid.

References

1. Primary and Remedial Cementing Guidelines. Drilling and Completions Committee, Alberta, April 1995. Distributed by the Petroleum Industry Training Service.
2. M.J. Economides, Implications of Cementing on Well Performance. In: E. B. Nelson (ed.), *Well Cementing*. Schlumberger Educational Services (1990) Chapter 1.
3. K. Newman, Cement pulsation improves gas well cementing. *World Oil*, July 2001 89–94.
4. B. Nichol, Choosing Economic Options for Shut-in Wells with a Risk Assessment Approach. Presentation at: *Cost-effective Abandonment Solutions, Technology Information Session*, Calgary May 3, 2000. Meeting organised by PTAC (Petroleum Technology Alliance Canada).
5. D. Dustrehoft, G. Wilson and K. Newman, Field Study on the Use of Cement Pulsation to Control Gas Migration. *Society of Petroleum Engineers* paper number SPE 75689 (2002).
6. R.H. McLean, C.W. Manry and W.W. Whitaker, Displacement Mechanics in Primary Cementing. *Society of Petroleum Engineers* paper number SPE 1488 (1966).
7. D. Guillot, H. Hendriks, F. Callet and B. Vidick, Mud Removal. In: E. B. Nelson (ed.), *Well Cementing*. Schlumberger Educational Services, (1990) Chapter 5.
8. C.F. Lockyear, D.F. Ryan and M.M. Gunningham, Cement Channelling: How to Predict and Prevent. *Society of Petroleum Engineers* paper number SPE 19865 (1989).
9. A. Jamot, Deplacement de la boue par le latier de ciment dans l'espace annulaire tubage-paroi d'un puits. *Revue Assoc. Franc. Techn. Petr.* 224 (1974) 27–37.
10. M. Couturier, D. Guillot, H. Hendriks and F. Callet, Design Rules and Associated Spacer Properties for Optimal Mud Removal in Eccentric Annuli. *Society of Petroleum Engineers* paper number SPE 21594 (1990).

11. S. Brady, P.P. Drecq, K.C. Baker and D.J. Guillot, Recent Technological Advances Help Solve Cement Placement Problems in the Gulf of Mexico. *Society of Petroleum Engineers* paper IADC/SPE 23927 (1992).
12. D.F. Ryan, D.S. Kellingray and C.F. Lockyear, Improved Cement Placement on North Sea Wells Using a Cement Placement Simulator. *Society of Petroleum Engineers* paper number SPE 24977 (1992).
13. V.C. Kelessidis, R. Rafferty, A. Merlo and R. Maglione, Simulator Models U-tubing to improve primary cementing. *Oil and Gas Journal*, March 7th 1994, 72–80.
14. S.H. Bittleston, J. Ferguson and I.A. Frigaard, Mud removal and cement placement during primary cementing of an oil well; laminar non-Newtonian displacements in an eccentric annular Hele-Shaw cell. *J. Engng. Math.* 43 (2002) 229–253.
15. M. Martin, M. Latil and P. Vetter, Mud Displacement by Slurry during Primary Cementing Jobs - Predicting Optimum Conditions. *Society of Petroleum Engineers* paper number SPE 7590 (1978).
16. A. Tehrani, J. Ferguson and S.H. Bittleston, Laminar Displacement in Annuli: A Combined Experimental and Theoretical Study. *Society of Petroleum Engineers* paper number SPE 24569 (1992).
17. A. Tehrani, S.H. Bittleston and P.J.G. Long, Flow instabilities during annular displacement of one non-Newtonian fluid by another. *Experiments in Fluids* 14 (1993) 246–256.
18. G.I. Barenblatt, V.M. Entov and V.M. Ryzhik, Theory of fluid flows through natural rocks. *Theory and Applications of Transport in Porous Media*, Volume 3. Dordrecht, Boston: Kluwer Academic Publishers (1990) 395pp.
19. R.V. Goldstein and V.M. Entov. *Qualitative Methods in Continuum Mechanics.* Harlow, Essex, England: Longman Scientific & Technical, New York: Wiley (1989) 279pp.
20. A.Kh. Mirzadjanzadeh, On a theoretical scheme of mud loss phenomenom. *Doklady AN Azerbaidjan SSR* 9 (1953) 203–205.
21. P.G. Saffman and G.I. Taylor, The penetration of a finger into a porous medium in a Hele-Shaw cell containing a more viscous liquid. *Proc. R. Soc. London* A245 (1958) 312–329.
22. P.G. Saffman, Viscous fingering in Hele-Shaw cells. *J. Fluid Mech.* 173 (1986) 73–94.
23. G.M. Homsy, Viscous fingering in porous media. *Ann. Rev. Fluid Mech.* 19 (1987) 271–311.
24. H. Pascal, Rheological behaviour effect of non-Newtonian fluids on dynamic of moving interface in porous media. *Int. J. Engng. Sci.* 22 (1984) 227–241.
25. H. Pascal, Dynamics of moving interface in porous media for power law fluids with a yield stress. *Int. J. Engng. Sci.* 22 (1984) 577–590.
26. H. Pascal, A theoretical analysis of stability of a moving interface in a porous medium for Bingham displacing fluids and its application in oil displacement mechanism. *Can. J. Chem. Engng.* 64 (1986) 375–379.
27. S.D.R. Wilson, The Taylor-Saffman problem for a non-Newtonian liquid. *J. Fluid Mech.* 220 (1990) 413–425.
28. V.A. Gorodtsov and V.M. Yentov, Instability of the displacement fronts of non-Newtonian fluids in a Hele-Shaw cell. *J. Appl. Maths Mech.* 61 (1997) 111–126.
29. P. Coussot, Saffman-Taylor instability in yield-stress fluids. *J. Fluid Mech.* 380 (1999) 363–376.
30. B. Dacoragna, *Direct Methods in the Calculus of Variations*. Berlin; New York: Springer-Verlag (1989) 305pp.
31. I. Ekeland and R. Temam, *Convex Analysis and Variational Problems.* Amsterdam: North-Holland Pub. Co.; New York, distributors for the U.S.A., American Elsevier Pub. Co. (1976) 402pp.
32. G. Duvaut and J.L. Lions, *Inequalities in Mechanics and Physics*. Berlin; New York: Springer-Verlag (1976) 397pp.
33. R. Glowinski, *Numerical Methods for Nonlinear Variational Problems.* New York: Springer-Verlag (1983) 493pp.
34. S. Pelipenko and I.A. Frigaard, Two-dimensional computational simulation of eccentric annular cementing displacements. Submitted to IMA J. Appl. Maths., January 2003, under review.